Science of the Total Environment 880 (2023) 163151

Contents lists available at ScienceDirect

Science of the Total Environment

journal homepage: www.elsevier.com/locate/scitotenv

Titanium-doped PET nanoplastics of environmental origin as a true-to-life model of nanoplastic

Aliro Villacorta [a,b], Lourdes Vela [a,c], Michelle Morataya-Reyes [a], Raquel Llorens-Chiralt [d], Laura Rubio [a], Mohamed Alaraby [a,e], Ricard Marcos [a,*], Alba Hernández [a,*]

[a] Group of Mutagenesis, Department of Genetics and Microbiology, Faculty of Biosciences, Universitat Autònoma de Barcelona, Cerdanyola del Vallès, Barcelona, Spain
[b] Facultad de Recursos Naturales Renovables, Universidad Arturo Prat, Iquique, Chile
[c] Faculty of Health Sciences Eugenio Espejo, Universidad UTE, Quito, Ecuador
[d] AIMPLAS, Plastics Technological Centre, Gustave Eiffel, 4, 46980 Paterna, Valencia, Spain
[e] Zoology Department, Faculty of Sciences, Sohag University, 82524 Sohag, Egypt

HIGHLIGHTS

- Nanoplastics from opaque PET milk bottles have been obtained.
- The hybrid (PET/TiO_2NPs) nature of this material has been demonstrated.
- TEM/confocal microscopy showed the colocalization of both constituents.
- TEM(*Ti*)NPLs internalize differentially according to the used cell types.
- No toxic effects were observed for this true-to-life NPL.

GRAPHICAL ABSTRACT

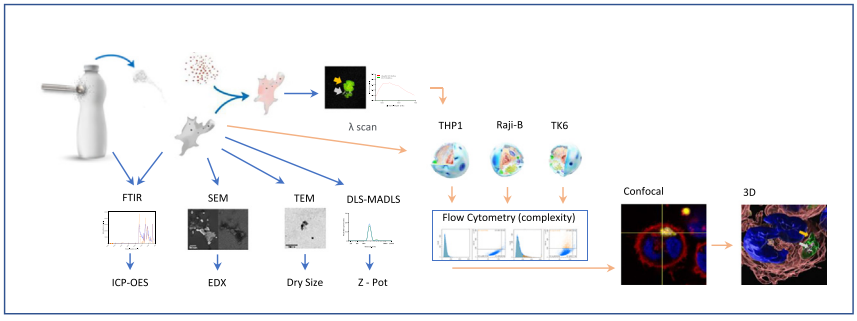

ARTICLE INFO

Editor: Damià Barceló

Keywords:
PET(Ti) nanoplastics
Obtention
Characterization
Cell internalization

ABSTRACT

The increased presence of secondary micro/nanoplastics (MNPLs) in the environment requires urgent studies on their potentially hazardous effects on exposed organisms, including humans. In this context, it is essential to obtain representative MNPL samples for such purposes. In our study, we have obtained true-to-life NPLs resulting from the degradation, *via* sanding, of opaque PET bottles. Since these bottles contain titanium (TiO_2NPs), the resulting MNPLs also contain embedded metal. The obtained PET(*Ti*)NPLs were extensively characterized from a physicochemical point of view, confirming their nanosized range and their hybrid composition. This is the first time these types of NPLs are obtained and characterized. The preliminary hazard studies show their easy internalization in different cell lines, without apparent general toxicity. The demonstration by confocal microscopy that the obtained NPLs contain Ti samples offers this material multiple advantages. Thus, they can be used in *in vivo* approaches to determine the fate of NPLs after exposure, escaping from the existing difficulties to follow up MNPLs in biological samples.

1. Introduction

The extended use of plastic goods has results in global environmental pollution by plastic wastes, and their consequent environmental alarms (Chang et al., 2022). Although plastics have a relatively long life, degradation occurs through different physical-chemical-biological processes generating the so-called micro- and nanoplastics (MNPLs). At these sizes, and especially at the nano range, MNPLs can be easily internalized by organisms

* Corresponding authors at: Group of Mutagenesis, Department of Genetics and Microbiology, Faculty of Biosciences, Universitat Autònoma de Barcelona, Campus of Bellaterra, 08193 Cerdanyola del Vallès, Barcelona, Spain.
E-mail addresses: ricard.marcos@uab.cat (R. Marcos), alba.hernandez@uab.cat (A. Hernández).

http://dx.doi.org/10.1016/j.scitotenv.2023.163151
Received 30 January 2023; Received in revised form 13 March 2023; Accepted 25 March 2023
Available online 1 April 2023

(including humans) following different routes, finally resulting in a potential health hazard (Rubio et al., 2020a; Gigault et al., 2021; Wu et al., 2022). Thus, determining the potential hazard risks associated with MNPLs exposure is a hot and current topic.

Although great efforts have been devoted to evaluating the hazards associated with MNPLs exposure, the lack of representative environmental MNPLs is a big barrier to overcome. Consequently, most of the studies have been carried out with pristine commercial polystyrene (PS) samples that, despite their advantages (uniformity, different sizes, surface functionalization, and fluorescent staining), are not fully representative of the environmental MNPLs (Xu et al., 2022). Although PSMNPLs have shown to be very useful for many purposes, the extrapolation of the obtained data is doubtful for human health risk assessment associated with MNPLs exposures (Brachner et al., 2020; Coffin et al., 2022). Consequently, the obtention of environmentally relevant (true-to-life) MNPLs is an urgent challenge to be achieved.

Due to the impossibility of getting enough uniform MNPLs just by picking up environmental samples, different protocols have been proposed by using the physical degradation of plastic goods, followed by the collection of the different fractions (containing MPLs or NPLs), and their ulterior characterization. Interestingly, most of the published proposals have used polyethylene terephthalate (PET) goods as the original source. This is mainly due to the high demand for this plastic type that is mainly used for packaging, including bottles for multiple purposes, although it is also a polymer widely used in the textile industry (PlasticsEurope, n.d.). Consequently, and because of the deficient recycling mechanisms and the lack of awareness on the part of society, they finally end up in the environment as plastic waste. Among the different experimental approaches, the UV-laser ablation process was first used to obtain PET-NPLs (Magrì et al., 2018). Alternatively, mechanical milling is another fractionation process used to obtain mainly the MPLs fraction (Astner et al., 2019; Pignattelli et al., 2021; Lionetto et al., 2021). Furthermore, the use of mechanical ground approaches has also been proposed as an easy way to obtain PET-NPLs (Rodríguez-Hernández et al., 2019; Roursgaard et al., 2022; Villacorta et al., 2022).

Among the different types of PET bottles, we can distinguish between transparent and opaque PET ones. Opaque PET bottles are highly used many for packing milk because they provide the light protection that UHT milk requires and minimize gas permeability which, together with their low cost, are some of their advantages in front of other packaging options (Tramis et al., 2021). These characteristics of the opaque PET are due to the presence of titanium dioxide nanoparticles (TiO_2NPs) used as a filler, which also allows for reducing the bottle thickness. One of the common protocols to increase the compatibility of the fillers introduced in the plastics intend to modify their surfaces by increasing their hydrophilicity or hydrophobicity. This compatibility critically depends on the particle size of the filler because that can increase/decrease viscosity affecting the physical and chemical properties of the final compound. Since surface treatments can decrease the viscosity of the compound or masterbatch, modifications of the surface of fillers are becoming important because of its improvement in adhesion (Mozetič, 2019). Surface modifications can be achieved by the chemical interaction of the fillers with compounds that possess functional groups, by chemical absorption on the surface of the particles of the filling material of some modifying agents, or by coating the filler particles with a suitable coupling agent (Fronza et al., 2019).

Aiming to obtain environmental representative MNPLs, we have used opaque PET bottles to obtain NPLs, following the protocol recently published (Villacorta et al., 2022). These true-to-life NPLs may help us to understand the complexity of the environmental MNPLs, while constituting unrivaled materials to be used to evaluate the potential health hazards of environmental MNPLs. Although different metals and metalloids like arsenic, cadmium, chromium (VI), and lead are normally used as plastic additives (Smith and Turner, 2020; Turner and Filella, 2021), they are present in amounts significantly less that TiO_2NPs in opaque PET bottles. The presence of such metals can suppose a potential concern from a toxicological perspective, not only for their possible leaching in environmental conditions but for their behavior in specific physicochemical conditions, such the acidic environments encountered in the digestive tract of many animals, when MNPLs are unintentionally ingested. Beyond their potential toxicological profile, the obtention of titanium-doped MNPLs can represent a suitable true-to-life model to follow up their fate in complex matrices, including experimental *in vivo* models. Before determining the potential toxicity of MNPLs exposure, their cell uptake must be demonstrated and, if possible, quantified. These aspects have been the subject of recent reviews considering both the exposure route and the model organism used (Paul et al., 2020; Huang et al., 2022; Dusza et al., 2023).

Here we present our approach to obtain PET(*Ti*)NPLs, as well as their complete physico-chemical characterization. In addition, preliminary data on their behavior in human cells under *in vitro* exposure conditions is also reported. It is important to point out that this is the first report getting and analyzing NPLs from opaque PET bottles.

2. Materials and methods

2.1. PET(Ti) nanoplastics obtention

We have used commercially available opaque-PET bottles to produce PET nanoplastics containing titanium [PET(*Ti*)NPLs]. The used procedure was based on the recently published method designed to get PETNPLs from water bottles (Villacorta et al., 2022). The process is schematized in Fig. 1. Briefly, pieces of about 12 cm^2 were cut from the original opaque PET bottle and sanded with a diamond rotary burr accessory, taking particular attention not to overheat the surface by passing in only one direction and only once on the same area. The obtained opaque PET debris was passed through a 0.20 mm sieve and 4 g of the resulting material was dispersed on 40 mL of trifluoroacetic acid pre-heated to 50 °C on a stirring plate at 100 rpm for 2 h and then kept under continuous agitation at room temperature overnight. The next day, 40 mL of TFA (20 %, v/v) were added and the mixture was kept under constant stirring for 24 h more. The suspension was then passed through the 0.20 mm sieve, to eliminate the bigger pieces, and centrifuged at 2500 rcf for 1 h once distributed on six 10 mL glass tubes. The obtained pellets were resuspended on 400 mL

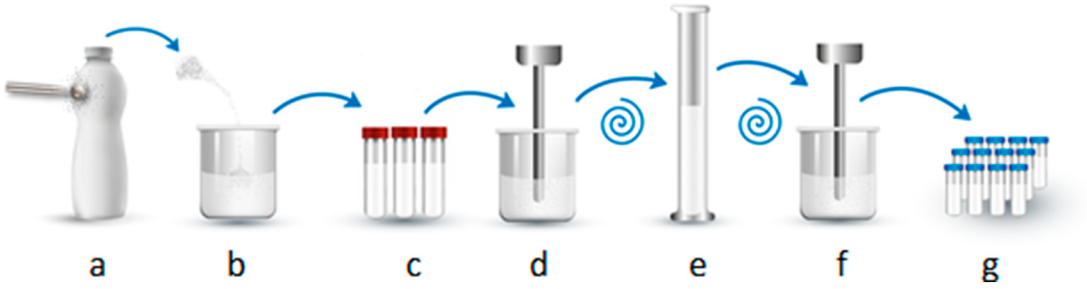

Fig. 1. Schematic representation of the PET(*Ti*)NPLs production. Opaque PET fragment from bottles were grinded until a powder is obtained, passed through the sieve (a), stirred, suspended, and heated at different concentrations of TFA (b), distributed on glass tubes and centrifuged (c), resuspended on SDS, sonicated (d), and transferred to a cylinder for sedimentation (e) and then collected, washed, weighted, resuspended and sonicated (f) and aliquots were prepared and stored frozen until needed (g).

of a 0.5 % sodium dodecyl sulfate (SDS) solution, vigorously mixed, distributed into two 200 mL beakers, and ultrasonicated on an SSE-1 Branson sonicator (Branson Ultrasonics Co., Brookfield, CT, USA) for 2 min at 25 % amplitude, in 9/9 s sonication/break cycles. The content of each beaker was transferred to a graduated cylinder to sediment for 1 h, to eliminate the bigger fraction. The top 100 mL of each cylinder were collected and centrifuged to eliminate SDS. Pellets were washed twice with Milli-Q water and twice with pure ethanol and dried under sterile air laminar flow. Pellets were then weighted and resuspended on Milli-Q water at concentrations of 10 mg/mL. Suspensions were then sonicated for 16 min at 10 % amplitude in a cold-water bath and stock solution aliquots of 1 mL were immediately frozen on cryotubes in liquid nitrogen and stored at −80 °C for further use.

2.2. PET(Ti)NPLs characterization by transmission electron microscopy (TEM)

A carbon-covered cooper grid was dipped into the working solution (200 μg/mL) and allowed to evaporate overnight. Particles in the grid were examined by TEM using a JEOL JEM 1400 instrument (JEOL Ltd., Tokyo, Japan) operated at 120 kV. TEM images were analyzed for particle size distribution by measuring the Martin diameter using the ImageJ software 1.8.0_172 and processed with the GraphPad Prism 7.0 software (GraphPad, San Diego, CA). The Savitzky-Golay-like filter was applied to smoothen the curve.

2.3. PET(Ti)NPLs characterization by scanning electron microscopy (SEM) & energy dispersive X-ray spectroscopy (EDS)

From the stock solution, a working solution of 200 μg/mL was prepared by thawing in a warm bath at 37 °C and diluted in Milli-Q water. The working solution was vigorously vortexed and 10 μL of the suspension were deposited on a silica holder. Water was evaporated from the sample and examined on an SEM Zeiss Merlin (Zeiss, Oberkochen, Germany) coupled with an X-Max 20 mm EDS system (Oxford Instruments, Oxford, UK). In addition to collecting SEM images, an area including the nanoparticle surface was selected for the EDX analysis, the signal was collected and analyzed by the INCA Energy software (INCA, Grinnell, IA, USA).

2.4. PET(Ti)NPLs characterization by multi-angle and dynamic light scattering (DLS-MADLS), and zeta potential

The indicative size of the colloid structures in the suspension of the PET (*Ti*)NPLs was determined using a Zetasizer® Ultra device from Malvern Panalytical (Cambridge, United Kingdom). To such end, a working solution of 100 μg/mL of PET(*Ti*)NPLs was used. Additionally, to investigate the influence of the culture media in the nanoplastic dispersion, the same concentration was prepared by using the Nanogenotox dispersion protocol (Nanogenotox, 2011), and its behavior was evaluated on both Milli-Q water and on FBS supplemented RPMI (Roswell Park Memorial Institute) medium supplemented with 10 % fetal bovine serum (FBS), 1 % glutamine (Biowest, France), and 2.5 μg/mL of PlasmocinTM 226 (InvivoGen, CA, USA).

2.5. PET(Ti)NPLs characterization by Fourier transform infrared spectroscopy (FTIR)

To detect functional groups, and to identify samples as PET, materials at different stages of the production process were used. Thus, pieces of original materials (water- and opaque-bottles), midterm production sanded material before acid exposure, and final nanoparticle samples were analyzed and compared. For PET(*Ti*)NPLs from the stock solutions (10 mg/mL), a drop was placed on a gold mirror and let dry for one week inside a Petri dish. For the solid samples, 3 × 3 cm pieces for both PET bottle types were cut directly from bottles. For the above-described materials (suspension and solids original samples), the analysis was carried out on a Vertex 80 device, while the dust of polymer-metal obtained from the sanded material was analyzed by using a Tensor 27 device. Both types of equipment were from Bruker (Bruker Corporation, Billerica, Massachusetts, USA). To assess the composition, the obtained interferograms were analyzed and contrasted with previously reported data.

2.6. PET(Ti)NPLs characterization by mass spectroscopy

To determine the Ti content of the original PET source, 0.10 g of the PET (Ti) film was weighted on a Mettler Toledo XP205DR analytical balance (Mettler-Toledo S.A.E., Barcelona, Spain). This amount was dispersed in Milli-Q water to the same concentration than the stock PET(Ti) (10 mg/mL). In an independent way, 0.25 mL of the two dispersions were vigorously agitated and digested in 5 mL of a mixture (4 mL HNO_3 65 % (p/v) and 1 mL of HF 40 % (p/v)) in a microwave oven for 20 min at 260 °C (ramp 25 min to reach 260 °C). Samples were diluted on HNO_3 (1 % v/v) before injection. The Ti content of the samples was determined on an inductively coupled plasma optical emission spectrometer ICP-OES Agilent 5900 (Agilent Technologies, Santa Clara, CA, USA).

2.7. PET(Ti)NPLs labeling and confocal visualization

To visualize/identify PET(*Ti*)NPLs on confocal microscopy, the reflection property was used for the detection of Ti. To visualize PET, separately from Ti, samples were labeled with iDye Poly Pink (iDye), following an adaptation of the published protocols to dye microplastics (Karakolis et al., 2019; Nguyen and Tufenkji, 2022). Briefly, a working solution of 1 mL of PET(*Ti*)NPLs at the concentration of 5 mg/mL was prepared from the stock dispersion (10 mg/mL) and transferred into a 1.5 mL tube containing previously weighed 0.01 g of the textile dye (iDye) used for synthetic fibers. The mixture was vigorously vortexed and incubated for 2 h at 70 °C on a glass tube. After cooling at room temperature, 9 mL of Milli-Q water was added to the suspension and then centrifuged at 4000 rpm on an Amicon® Ultra-15 centrifugal Ultracel®-100 K filter 1×10^5 MWCO for 15 min. This step was performed twice to remove the excess of iDye. The washed particles were then collected and suspended in the final volume of 1 mL of Milli-Q water and stored protected from light at 4 °C until needed. Here on, these stained PET(*Ti*)NPLs are named iDyePET(*Ti*)NPLs. For their visualization in the confocal microscope, the particle suspension was diluted on Milli-Q water at a final concentration of 400 μg/mL and two drops of 20 μL were placed on a slide, covered with a coverslip, and let dry inside the biosafety cabinet on air laminar flow. PET(*Ti*)NPLs were prepared similarly to be used as control. Both slides were examined by confocal microscopy using a Leica TCS SP5 confocal microscope. Excitation wavelength of 561 nm was set on an acousto-optic tunable filter (AOTF 561) and, emission spectra was collected between 580 and 700 nm (lambda scan begin bandwidth 575.00–585.00 nm to lambda scan end bandwidth 691.00–701.00 nm). Emission was analyzed using the Leica Application Suite X 3.7.5.24914 (Leica Microsystems CMS GmbH Wetzlar, Germany). Images were collected under the same conditions, further explained on Section 2.10.

2.8. Cell culture

To determine the cell internalization ability of PET(*Ti*)NPLs, three human hematopoietic cell lines were used. Thus, THP-1 monocytes, TK6 lymphoblasts, and Raji-B B-lymphocytes were selected as a widely distributed and accepted lymphoblastic human cell models. All three cell lines were purchased from Sigma Aldrich (MO, USA). Cells were grown in T-25 flasks on RPMI medium (Biowest, France) supplemented with 10 % FBS, 1 % glutamine (Biowest, France), and 2.5 μg/mL of Plasmocin (InvivoGen, CA, USA). Cultures, with a density ranging from 5×10^5 to 1×10^6 cells, were maintained at 37 °C in a humidified atmosphere of 5 % CO_2.

2.9. PET(Ti)NPLs cell uptake (internal complexity), as determined by flow cytometry

To quantify cell internalization, the internal complexity of the exposed cells was used as an indicator of internal structural cell complexity and

determined by flow cytometry. To proceed, the three selected cell lines (TK6, Raji-B, and HTP-1) were grown on U-bottom 96 well plate at a cell density of 5×10^5 cells/mL on a final volume of 0.20 mL and treated with concentrations of 25, 50, and 100 μg/mL for a 24 h period. Once PET(*Ti*)NPLs uptake takes place, the orthogonal light scattering – commonly known as Side Scatter (SSC) – was evaluated using a flow cytometer Cytoflex S (Beckman Coulter CytoFLEX S). A total number of 10,000 events (single cells) were scored and evaluated using the CytExpert software and data was processed using GraphPad Prism Software 7.0. (GraphPad, San Diego, CA).

2.10. PET(Ti)NPLs cell uptake determination by confocal microscopy

For the visualization of internalized PET(*Ti*)NPLs into the cells, confocal microscopy was used using the protocol recently described (Annangi et al., 2023). Nuclei were stained using Hoechst 33342 (excitation of 405 nm and emission collected at 415–503), and cell membranes were dyed using Cellmask (excitation of 633 nm and emission collected at 645–786). For iDyePET(*Ti*)NPLs, an excitation wavelength of 561 nm and emission collected at 570–630 were used. For the localization of Ti, reflection images were obtained in parallel. Images of each sample were obtained using a Leica TCS SP5 confocal microscope and processed using ImageJ processing and analysis software, version 265 1.8.0_172.

2.11. Cell viability effects of PET(Ti)NPLs in the used cell lines

To assess the cell viability of the three hematopoietic cell lines after exposure, cells were seeded on the same conditions as previously described at a cell density of 5×10^5 cells/mL on a final volume of 0.20 mL on U-bottom 96 well plates and treated with concentrations ranging from 0 to 100 μg/mL for a 24 h period at standard conditions. Cells were then mixed and diluted 1:100 on ISOFLOW and counted with a ZTM coulter counter (Beckman Coulter Inc., CA, USA. The average number of cells counted on each treatment was compared with the average number of the untreated control cells and data was evaluated using GraphPad Prism Software 7.0. (GraphPad, San Diego, CA).

3. Results and discussion

The PET(*Ti*)NPLs samples obtained according to the protocol outlined in Fig. 1 were used for further characterization. It should be remarked the large amount of material obtained in the extraction process above described. The resulting 10 vials of 1 mL of the stock dispersion (10 mg/mL) were stored at −80 °C. Working solutions were prepared following the Nanogenotox protocol and aliquoted in 10 vials containing 0.2 mL of a concentration of 5000 μg/mL. This means that a standard PET(*Ti*)NPLs production generate 100 vials of the working dispersion, which were stored at the same conditions until used. This is a large amount that permit to carry out several rounds of studies aiming to perform a complete characterization and they hazard evaluation. The original process (Villacorta et al., 2022) has been used several times from PET water bottles to get more material to be spread among the PlasticHeal consortium, showing a very high repeatability.

3.1. Dry state size distribution and shape

TEM was used to determine the morphology and the size of the obtained PET(*Ti*)NPLs. The obtained figures were compared with those previously obtained from transparent PET bottles (Villacorta et al., 2022). In Fig. 2 it is indicated the morphology of PETNPLs (a) as compared with PET(*Ti*) NPLs (b and c). As observed, it is relatively easy to detect differences on the electrodensity of the sample when Ti is present. The presence of TiO_2NPs results in high-density points. Obviously, the degree of agglomeration can also be a factor modulating density. When the Martin diameter was measured for more than one hundred PET(*Ti*)NPLs figures, a mean size of 382.07 nm with a polydispersity index of 0.37 was obtained. Interestingly, the high electrodensity of TiO_2NPs also permitted to determine their size distribution inside the PET(*Ti*)NPLs complex, as indicated in Fig. 2d.

From the size distribution it is obvious that the average exceeds the range of the nanoparticles (or by extension of a nanoplastic) definition. The last recommendation of the European Commission state that, at least the 50 % of the particles contained in a dispersion must be in the nano-range, and at least one dimension must be in the 1–100 nm range (European Commission (EC), 2022). Nevertheless, this definition looks appropriated for the engineered nanomaterials, and by extension for the primary nanoplastics, but not seems adequate for secondary nanoplastics resulting from the degradation of macroplastic goods, were a large range of sizes and shapes are expected. To describe the new true-to-live obtained nanoplastics we propose to take into consideration the proposal of Hartmann et al. (2019). These authors propose to categorize MNPLs according to the conventional units of size: nano (1–1000 nm) and micro (1–1000 μm). Although the authors divide the nano range between nanoplastics (1–100 nm) and submicron-plastics (100–1000 nm), this division add more darkness than light. Thus, from the operational point of view our sample of PET(*Ti*)NPLs distribution falls into the nano range.

3.2. Dry state morphology and composition

To better identify the PET(*Ti*)NPLs morphology and composition, SEM-EDS methodologies were used. Fig. 3a and b show the observed morphologies. It must be noted that due to the high electrodensity of Ti, the morphological visualization of PET is affected, and the figure definitions are not optimal. It is important to note the morphology of the TiO_2NPs showing their nanorod shape. Considering the average length of the TiO_2NPs nanorod present in the PET(*Ti*)NPLs it is assumable the size distribution determined by TEM, since it is difficult to find PET structures not associated to TiO_2NPs.

As previously indicated, different metals and metalloids like arsenic, cadmium, chromium (VI), and lead are normally used as plastic additives

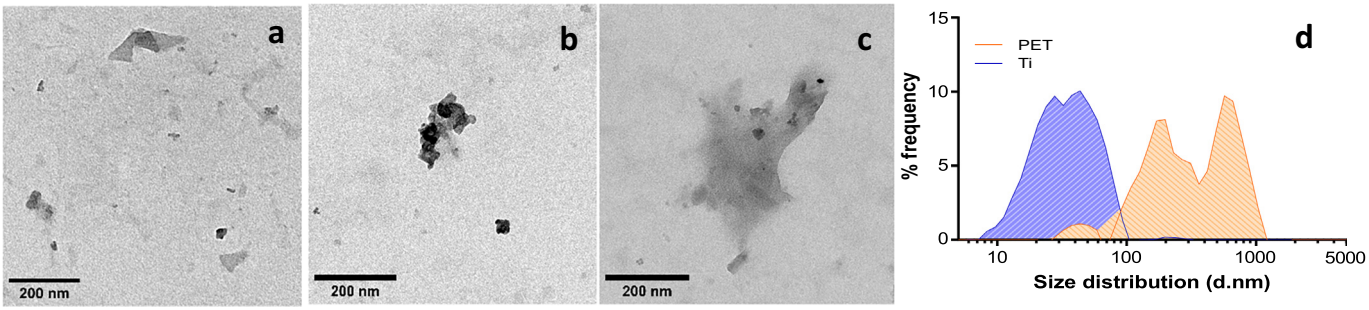

Fig. 2. TEM figures from in-house secondary PETNPLs (a) compared with PET(*Ti*)NPLs (b, c). The presence of TiO_2NPs is detected as a high density spots. Size distribution for PET(*Ti*)NPLs was determined, and a bimodal distribution was observed (orange). Due to the good detection of TiO_2NPs, their size distribution (Martin diameter) was also determined (blue).

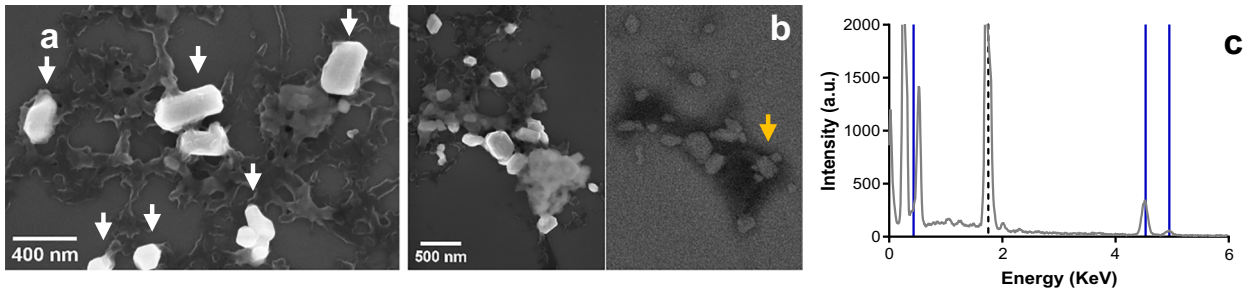

Fig. 3. SEM figures of PET(*Ti*)NPLs show TiO_2NPs embedded on nano-PET structures both on secondary electrons view (a), and both secondary (b, left) and backscattered (b, right) electrons. On (a) the white arrows indicate the TiO_2NPs, and on (b) the yellow arrow indicates the TiO_2NPs that are not easily visible due to the polymer covering. The EDS spectrum observed on (c), show the characteristic peaks of Ti remarked on blue, and the dashed line indicates the Si holder interference.

and, consequently, they can be found in their derived MNPLs (Turner and Filella, 2021). Nevertheless, the levels of titanium present in the MNPLs resulting from opaque bottles, like the obtained in this study, are very much high and impregnating the resulting MNPLs. This could suppose an associated hazard risk for such type of MNPLs. It should be remembered that Ti compound, and by extension TiO_2NPs, is a recognized food additive (E171), wide used in many food matrices (Cornu et al., 2022), were the E letter codes for substance that can be used as food additives. In addition to the multiple studies looking for potential hazards associated with E171 use, a recent publication from the panel on Food Additives and Flavorings from the European Food Safety Authority (EFSA) indicates that, "based on all the evidence available, E171 can no longer be considered as safe when used as a food additive" (EFSA Panel on Food Additives and Flavourings (FAF) et al., 2021).

Nevertheless, PET(*Ti*)NPLs samples can result very useful for specific purposes. The need to detect the fate of MNPLs in complex environmental matrices has been outlined as a special challenge. In the same way, to determine the fate of MNPLs in complex organisms like mammals is another important challenge. To overcome this problem, the use of metal-doped nanoplastics has been proposed (Mitrano et al., 2019; Clark et al., 2022). Nevertheless, these type of nanoplastics are far from the representative secondary MNPLs present in the environment. From this point of view our PET (*Ti*)NPLs would cover two main aspects, i) are MNPLs containing metal that can be used to determine their fate in experimental mammalian models, and ii) are true-to-life representative environmental MNPLs.

3.3. PET(Ti)NPLs size distribution and zeta potential in aqueous solution

The hydrodynamic behavior of PET(*Ti*)NPLs dispersed on Milli-Q water, or following the Nanogenotox protocol, shows mild differences among them. Independently of these mild differences, they show that there is a need of standardized procedures when it comes to nanoplastic dispersions. At this point is relevant to point out that, independently of the dispersion used, all obtained values do not differ importantly from the values obtained when TEM approaches were used (382.07 nm).

As observed on Fig. 4a–d, in terms of size distribution in number percentage, the curves whether on water or RPMI supplemented media almost overlap, and the *Z*-average shows no significant differences except for the behavior of PET(*Ti*)NPLs on supplemented RPMI, when compared with water dispersion using the one-way ANOVA with Dunnett multiple comparison test with a significance of 0.05. These data indicate that the surface coating of the particles is relevant in terms of hydrodynamic behavior when complex matrices must to be used. This not only apply for *in vitro* studies but mainly for *in vivo* studies, pointing out the need of stablish

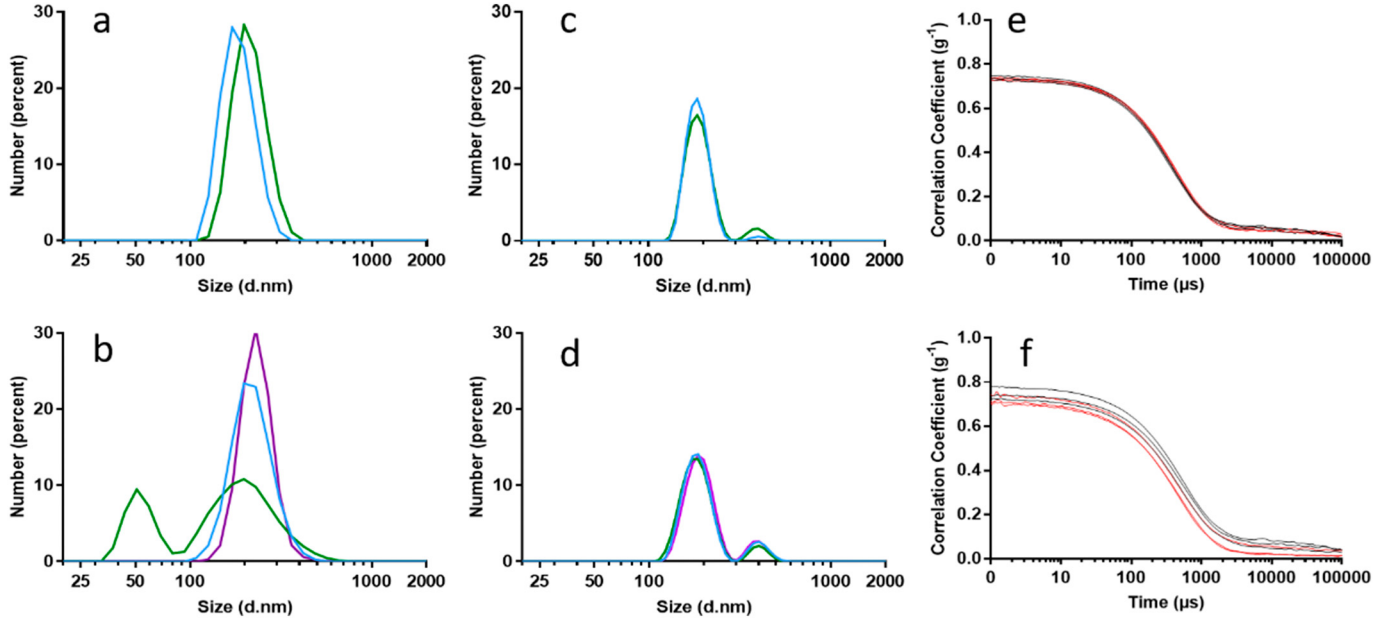

Fig. 4. Size distribution analysis of PET(*Ti*)NPLs on MiliQ water (a, c) and on supplemented RPMI media (b, d) are shown by DLS (a, b) and (MADLS) (c, d) on Milli-Q water (light blue line on all charts) and on the Nanogenotox dispersion protocol (green line on all charts). Additionally multiple narrows measurements (purple lines on b and d) are shown. All correlation measurements are shown at the right side of the corresponding line (e, f, respectively).

Table 1
Description of hydrodynamic measurements.

Sample	*Z*-average	PDI	Z-potential*
PET(*Ti*)NPLs — Milli-Q	308.00 ± 6.10	0.36	−33.10 (1)
PET(*Ti*)NPLs — Nanogenotox	320.00 ± 8.18	0.34	−18.23 (2)
PET(*Ti*)NPLs – RPMI – Nanogenotox	287.00 ± 16.10	0.40	−9.51 (3)
PET(*Ti*)NPLs — RPMI	357.00 ± 36.50$^{\times}$	0.41	−6.96 (4)

* Significant differences in Z-potential values were determined by the one-way ANOVA analysis, with a Tukey's multiple comparison test. Comparisons were established between dispersion conditions (1–4) as follows: (1–2**) (1–3***), (1–4***), (2–3*), (2–4*), and (3–4^{ns}). [ns: non-significant; *$P < 0.05$, **$P < 0.01$; ***$P < 0.001$]. x significant (P<0.05) in comparison with Milli-Q water dispersion.

implemented dispersion protocols of nanoplastics as a good practice in terms of keeping the dispersed nanoplastics in the nanoscale range. This is a relevant key factor when different biological endpoints must be further tested. The differences in the *Z*-average when the BSA is added to the PET (*Ti*)NPLs dispersion and tested on supplemented RPMI culture medium may result in an electrosteric stabilization and this can be depicted not only in the already described changes but also in the *Z*-potential differences (Table 1) where the surface charge of the particle is dramatically shifted. In terms of significance, and regarding the Z-potential values, only PET(*Ti*) NPLs suspended on RPMI with or without the Nanogenotox protocol are not significantly different. When water dispersion values are compared with the other dispersion protocols, very significant differences for Z-potential values are observed. The particles dispersed in complex matrices tend to present a higher value of heterogeneity, which can be confirmed by observing that the values of this type of dispersion are above 0.40 in terms of the polydispersity index (PDI), while the dispersions in water do not exceed this value. In both cases, the values are not excessively low.

3.4. Chemical determination of the PET(Ti)NPLs and Ti content quantification

As the FTIR methodology is suitable for the analysis of films, suspensions, and powders, we have used this tool to confirm the chemical identity of our PET(*Ti*)NPLS. This approach was used not only for the characterization of the final nanomaterial product, but also for the original commercial material (opaque PET films) and for the PET(Ti) powder obtained in the mid-step part of the process of our PET(*Ti*)NPLS generation. The main reason of this sequential analysis was to demonstrate that not changes in the original chemical (PET) nature was produced in the nano PET obtaining process. As observed in the Fig. 5 no significant differences in the obtained spectra are observed, confirming that the different steps carried out in the process does not modify the PET chemical nature. Thus, we can observe how the simultaneous determination of the organic component of the sample are consistent and correspond with the spectra of PET previously reported on literature (Chen et al., 2013; Johnson et al., 2021), as well as in our previous work (Villacorta et al., 2022).

As a control, regular commercially available PET samples, as well as the nanoparticles produced from their degradation are also presented (Figs. 5a, b). We assume that during the degradation process, a fraction of the original material is lost. We specifically ask if part of the titanium content could be lost during the process. To such end we determined the percentage of titanium in the original film and in the resulting nanoplastic. Results indicate that the titanium content of the opaque PET films was 3.83 %, which was reduced to 2.60 % in the resulting PET(*Ti*)NPLs. Results for ICP-OES for the resulting PET(*Ti*)NPLs were very consistent and the variability among replicates was low, never been higher than 1 μg/mL, and the relative standard deviation (RSD) was never higher than 7 %. On the other hand, for opaque PET film, the differences among replicates were never higher than 0.1 mg/g and the RSD was never higher than 0.6 %. We assume that during the different ultracentrifugation steps, some titanium (possibly due to its high weight) is lost. Nevertheless, a very important fraction remains associated to the final product of the degradation process. Although no indications on the potential leakage of titanium from the opaque bottles have been found, such plastic can suppose many problems entering in the recycling processes (Tramis et al., 2021).

3.5. PET(Ti)NPLs labeling and confocal visualization

In this study we successfully dye PET(*Ti*)NPLs with the commercially available textile dye *iDye Poly Pink* by heating the nanoplastic/dye mixture allowing the swelling of the polymer at the time that allowing the dye entering the polymeric matrix, achieving that within the polymeric matrix we can find both the titanium and the iDye. Particles were then resuspended and washed on Milli-Q water to remove the excess of pigment not attached to the particles, as previously described and depicted on Fig. 6a. iDyePET(*Ti*)NPLs shows a significant amount of fluorescence easily observed by confocal microscopy where fields with significant particle agglomerates were located and the emission collected (Fig. 6b, c, d). Consistent with previous reports (Karakolis et al., 2019) the fluorescence on PET was easily observed by this staining approach with the main difference that in our study we use nanoplastic instead of microplastics. In a recent study, authors shows that a commercially available dye (Atto 647N) can be used for similar approaches to stain different pristine NPLs (Nguyen and Tufenkji, 2022). It is necessary to remark that in our approach, in house made true-to-life nanoplastic have been used showing the suitability of our method not only for the type of polymer but also for size differences,

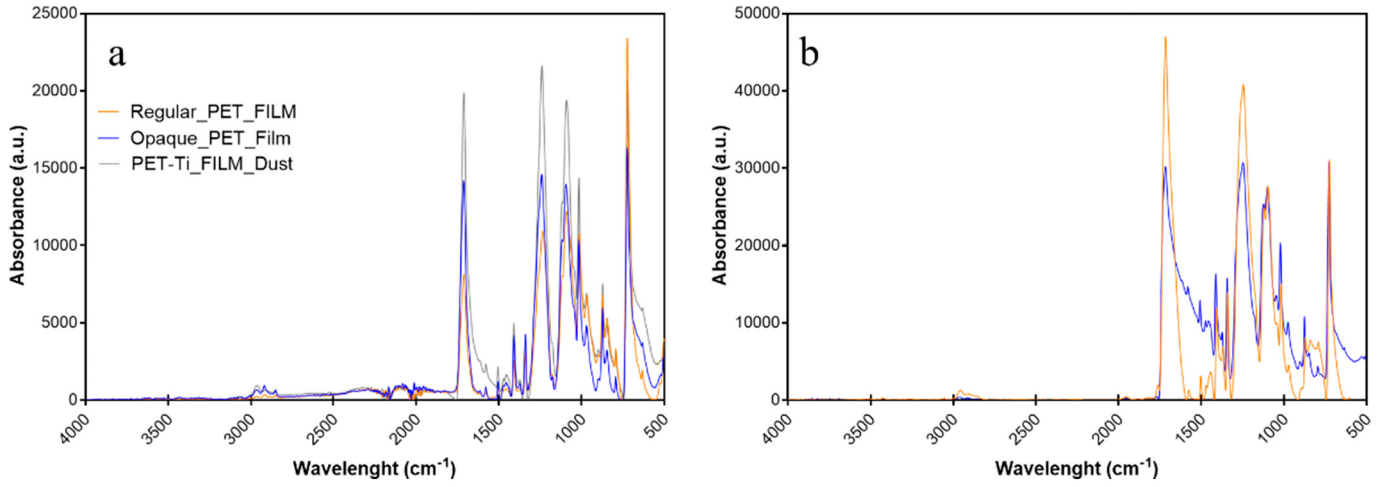

Fig. 5. FTIR spectra of the principal peaks of the interferogram. On the left chart (a) regular (orange), opaque PET (blue), and opaque PET dust produced from degradation process spectra are shown. On the right chart (b) PETNPLs (orange) from regular PET film and PET(*Ti*)NPLs (blue) from opaque PET are shown.

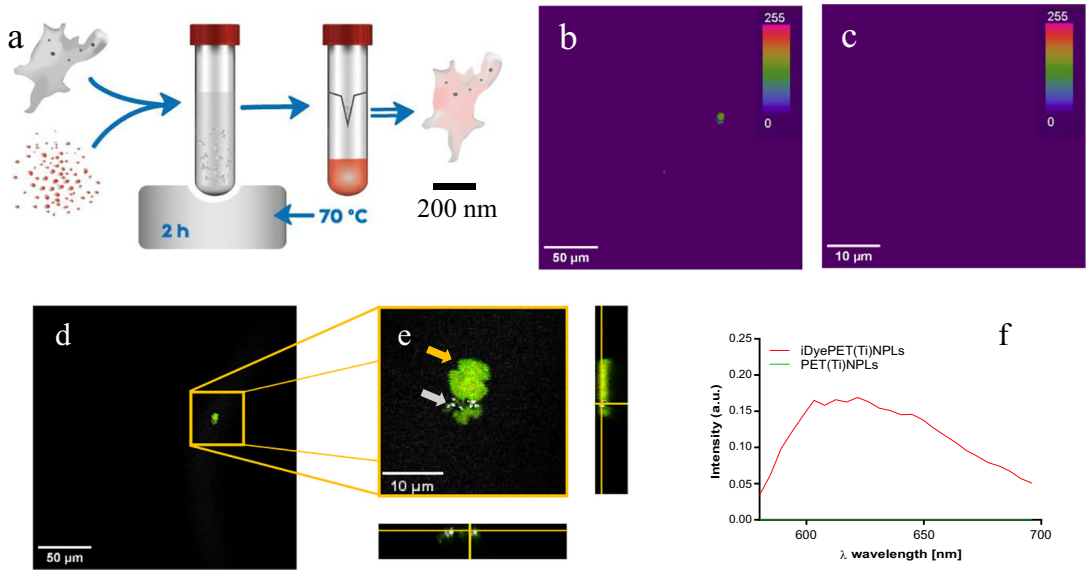

Fig. 6. a) Staining procedure: PET(*Ti*)NPLs were mixed with iDye Poly pink and heated at 70 °C for 2 h, then filtered, and finally resuspended. Labeling was evaluated by confocal microscopy acquiring images of the fluorescence where iDyePET(*Ti*)NPLs and PET(*Ti*)NPLs were observed agglomerated (b, c, respectively). d) When the signal for both iDye (yellow arrow) and Ti (grey arrow) were used, both signals appear together as indicative of the PET(*Ti*)NPLs identification. f) The emission spectra for both particles were collected and compared (green signal overlap the X-axis).

due to the polydisperse nature of our material. As shown in Fig. 6d, signals corresponding to PET and Ti co-localize, demonstrating the mixed nature of PET(*Ti*)NPLs. Finally, no fluorescence signal for iDye was detectable on fields were PET(*Ti*)NPLs were the only component.

3.6. Cellular uptake evaluation

The potential harmful effects induced by MNPLs exposure require their previous internalization. There are different approaches to measure such uptake, and in this study we have used both flow cytometry and confocal microscopy. By using flow cytometry, the intensity of the side-scattered light revealed that the particles were taken up in the cells, as initially proposed (Suzuki et al., 2007). This method has been used to detect the uptake of different nanomaterials including titanium nanoparticles, by measuring the complexity of the BEAS-2B cells (Vales et al., 2015). In our study, this method has been applied to different hematopoietic cell lines to determine potential differences according to the used cell type. If MNPLs can cross the protective barriers, they move to the general compartment (blood), interacting with their respective components. Thus, blood cells can be considered as a general target to be used to determine the potential effects of any exposure including MNPLs and more specifically PET(*Ti*)NPLs. The obtained results are indicated in Fig. 7, for three well-known leukocytic cell lines: TK6 lymphoblastic, Raji-B lymphocytes, and THP-1 monocytic cells (Rubio et al., 2020b). As observed, the PET(*Ti*)NPLs uptake differs among the cell lines, leukemic monocytes (THP-1) showing the highest increase on cell complexity after exposures lasting for 24 h, and at all tested concentrations. Contrary, the lymphoblastic TK6 show practically no uptake. This differential uptake was also reported for polystyrene NPLs using the same leukocytic cells (Rubio et al., 2020b), as well as for three different white peripheral blood cells (lymphocytes, monocytes, and polymorphonuclear cells) (Ballesteros et al., 2020). Accordingly, the complexity of the uptake response must be considered in the selection of the cells to be used in any experiment aiming to evaluated hazardous effects of MNPLs.

As indicated, cell uptake can also be determined by using confocal microscopy, as observed in Fig. 8. For this approach we focus our attention on THP-1 cells since this cell line showed the highest uptake in the flow cytometry approach. Interesting, we could colocalize both the signal coming from the emission of the iDye on the iDyePET(*Ti*)NPLs and the signal from Ti. This is observed when Fig. 8b and c are compared, indicating the *hybrid* composition of the obtained PET(*Ti*)NPLs. The orthogonal views confirm the complex structures previously observed by using electronic microscopy (whether transmission or scanning) but this time inside a cell, as expected according to the complexity results obtained by flow cytometry. It is necessary to point out that not all the Ti remains attached to the PET MNPLs, since a fraction of the total is lost during the obtention process, as we describe on the Section 3.4, and quantify by ICP-OES. Nevertheless, the colocalization signals give relevant information supporting the mixed nature of the obtained true-to-life PET(*Ti*)NPLs.

3.7. PET(Ti)NPLs effects on cell viability

As a final approach in the exhaustive evaluation of the characteristics of the obtained true-to-life PET(*Ti*)NPLs, the harmful effects in different human cell lines were determined in terms of cell survival. The obtained results are depicted in Fig. 9.

Despite the previous results, showing notorious differences on the uptake among the different selected cell lines, no significant decreases on cell viability were noticeable for any tested concentration nor cell line. This would confirm that the obtained true-to-life NPLs are not toxic, at

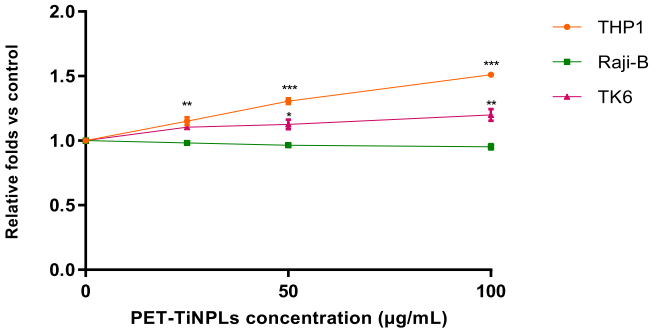

Fig. 7. Cellular internalization of PET(*Ti*)NPLs by Raji-B, TK6, and THP-1 cells after exposures lasting for 24 h. Graphs show the mean ± SEM of three different experiments performed in duplicates. Complexity was compared with untreated cells using a One-way ANOVA analysis with Dunnett multiple comparisons post-test. (**$P < 0.01$; ***$P < 0.001$).

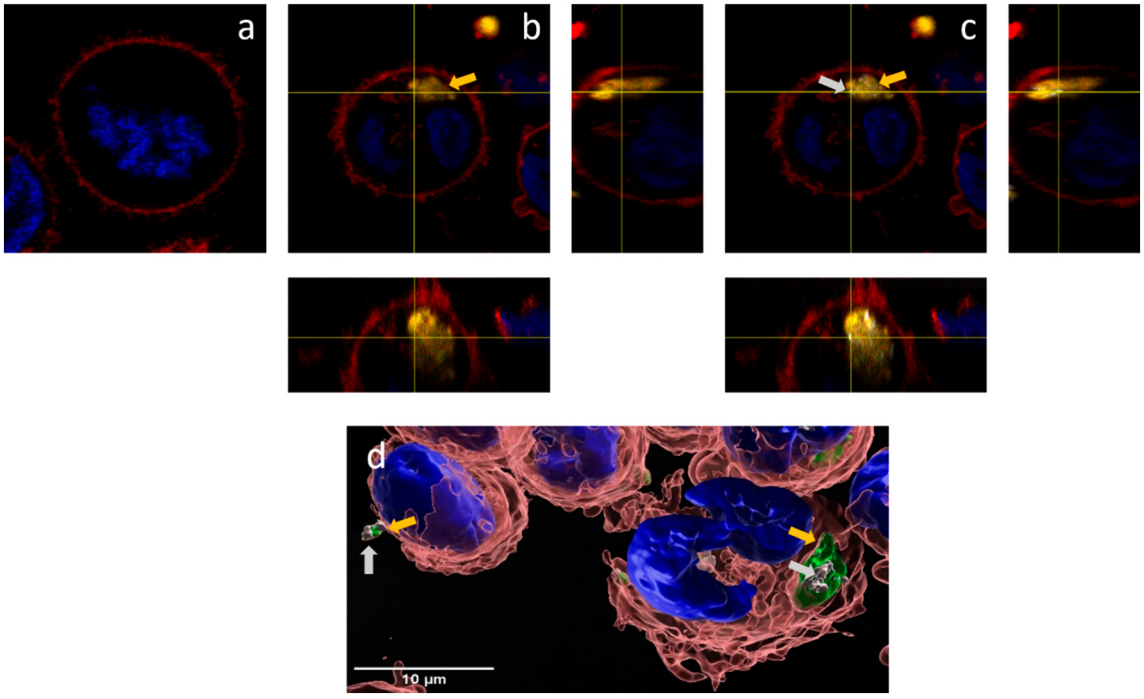

Fig. 8. Confocal microscopy uptake detection of iDyePET(*Ti*)NPLs in THP-1 cells, following 24 h exposure to 100 μg/mL. a) Control, untreated cells. b) Orthogonal view of THP1 cell with the Ti nanoparticles channel off and showing only iDye signal (yellow arrow). c) Co-localization of the Ti signal (grey arrow) with the PETNPLs emission. Arrows indicate both iDye and Ti signals. d) Imaris image reconstruction.

least in the used hematopoietic cell lines and detecting effects on cell viability. This would agree with previous experiments exposing these cell lines to polystyrene nanoparticles, where not viability effects were observed in that range of exposures lasting for 24 h, and only mild effects when concentrations range to high levels such as 200 μg/mL (Rubio et al., 2020b). The lack of effects on cell viability of PET(*Ti*)NPLs is like our previous report using true-to-life PETNPLs obtained from sanding water bottles material (Villacorta et al., 2022), and from other secondary nano PET particles obtained following other degradation procedures (Magrì et al., 2018; Dhaka et al., 2022). Although the PET component is not considered as potentially toxic, what about the other component (TiO_2NPs)? It should be remembered that TiO_2NPs were authorized as a food additive (E171) in the EU, according to Annex II of Regulation (EC) No 1333/2008. A recent review conducted by the European Food Safety Authority (EFSA) on the safety of

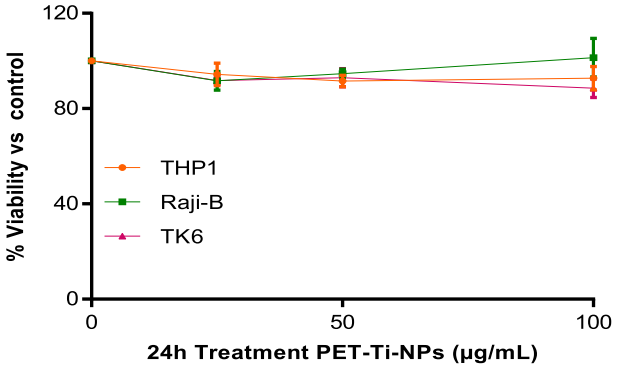

Fig. 9. Viability of hematopoietic THP-1, TK6, and Raji-B cells after exposures to PET(*Ti*)NPLs at concentrations ranging from 0 to 100 μg/mL for 24 h. The graph represents the viability relative to untreated cells. Graphs show the mean ± SEM of three different experiments performed in duplicates. One-way ANOVA analysis with Dunnett multiple comparisons post-test with a confidence level of 95 % was performed.

TiO_2NP used as food additive concluded that not toxic/harmful were identify, but a concern on their potential genotoxicity cannot be ruled out (EFSA Panel on Food Additives and Flavourings (FAF) et al., 2021). Accordingly, our data would agree with the assumed non-harmful effects of PET(*Ti*) NPLs exposure. It is obvious that cell viability is just the first step in the evaluation of the potential toxicity of PET(*Ti*)NPLs. Consequently, further extensive studies using a wide set of biomarkers are required to ruled out the existence of any type of harmful effects associated to the secondary MNPLs resulting from the degradation of opaque plastic goods.

4. Conclusions

True-to-life representative MNPLs, resulting from the degradation of environmental plastic waste, are urgently required to be used as a model for determining their potential hazards. In this context, the content of this study reports the obtention and characterization of MNPLs resulting from the degradation of opaque milk plastic bottles [PET(*Ti*)NPLs] which contain TiO_2NPs. This is the first study reporting the obtention/characterization of this type of MNPLs. In addition to the multiple physicochemical assays determining the hybrid chemical nature of the obtained material, size and shape confirmed their nano range size. The preliminary studies on their biological effects show an important but variable cell uptake, depending on the used cell line. Although no significant cell viability effects were observed in any of the used cell lines, further and complex studies are necessary to have a clear view of their potential health hazards. It must be pointed out that confocal microscopy images reported that both, in the dispersion media or internalized inside the cells, PET and Ti signals colocalize. This offers an important advantage to the obtained NPLs since they can be used in *in vivo* studies to demonstrate their fate inside the organism, thanks to the easy identification/localization/quantification of internalized Ti.

CRediT authorship contribution statement

RM and AH planned the experiments. AV, LV, MMR, RLC, LR, and MA carried out the experimental part. AV analyzed the data, carried out the

statistical analysis, and prepared tables/figs. AV, RM, and AH wrote the final manuscript.

Data availability

Data will be made available on request.

Declaration of competing interest

The authors declare that they have no known competing financial interests or personal relationships that could have appeared to influence the work reported in this paper.

Acknowledgments

A. Villacorta was supported by PhD fellowships from the National Agency for Research and Development (ANID), CONICYT PFCHA/DOCTORADO BECAS CHILE/2020-72210237. L. Vela was supported by PhD fellowships from the Fundación Carolina. L. Rubio hold a postdoctoral Juan de la Cierva contract (IJC2020r2686I/AEI/10.13039/501100011033). M. Alaraby hold a Maria Zambrano postdoctoral contract (code 693063) from the Spanish Ministerio de Universidades, funded by the European Union-Next GenerationEU, at the UAB. M. Morataya-Reyes hold a Ph.D. FI fellowship from the Generalitat de Catalunya, A. Hernández was granted an ICREA ACADEMIA award.

This project has received funding from the European Union's Horizon 2020 research and innovation programme under grant agreement No 965196. This work was partially supported by the Spanish Ministry of Science and Innovation (PID2020-116789, RB-C43) and the Generalitat de Catalunya (2021-SGR-00731).

We thank the Molecular Inorganic Nanoparticles Group at the *Institut Català de Nanociència i Nanotecnologia* (ICN2-UAB-CSIC-BIST) at the UAB campus for using their premises.

References

Annangi, B., Villacorta, A., López-Mesas, M., Fuentes-Cebrian, V., Marcos, R., Hernández, A., 2023. Hazard assessment of polystyrene nanoplastics in primary human nasal epithelial cells, focusing on the autophagic effects. Biomolecules 13, 220. https://doi.org/10.3390/biom13020220.

Astner, A.F., Hayes, D.G., O'Neill, H., Evans, B.R., Pingali, S.V., Urban, V.S., Young, T.M., 2019. Mechanical formation of micro- and nano-plastic materials for environmental studies in agricultural ecosystems. Sci. Total Environ. 685, 1097–1106. https://doi.org/10.1016/j.scitotenv.2019.06.241.

Ballesteros, S., Domenech, J., Barguilla, I., Cortés, C., Marcos, R., Hernández, R., 2020. Genotoxic and immunomodulatory effects in human white blood cells after ex vivo exposure to polystyrene nanoplastics. Environ. Sci. Nano 7, 3431–3446. https://doi.org/10.1039/d0en00748j.

Brachner, A., Fragouli, D., Duarte, I.F., Farias, P.M.A., Dembski, S., Ghosh, M., Barisic, I., Zdzieblo, D., Vanoirbeek, J., Schwabl, P., Neuhaus, W., 2020. Assessment of human health risks posed by nano-and microplastics is currently not feasible. Int. J. Environ. Res. Public Health 17 (23), 8832. https://doi.org/10.3390/ijerph17238832.

Chang, X., Fang, Y., Wang, Y., Wang, F., Shang, L., Zhong, R., 2022. Microplastic pollution in soils, plants, and animals: a review of distributions, effects and potential mechanisms. Sci. Total Environ. 850, 157857. https://doi.org/10.1016/j.scitotenv.2022.157857.

Chen, Z., Hay, J.N., Jenkins, M.J., 2013. The thermal analysis of poly(ethylene terephthalate) by FTIR spectroscopy. Thermochim. Acta 552, 123–130. https://doi.org/10.1016/j.tca.2012.11.002.

Clark, N.J., Khan, F.R., Mitrano, D.M., Boyle, D., Thompson, R.C., 2022. Demonstrating the translocation of nanoplastics across the fish intestine using palladium-doped polystyrene in a salmon gut-sac. Environ. Int. 159, 106994. https://doi.org/10.1016/j.envint.2021.106994.

Coffin, S., Bouwmeester, H., Brander, S., Damdimopoulou, P., Gouin, T., Hermabessiere, L., Khan, E., Koelmans, A.A., Lemieux, C.L., Teerds, K., Wagner, M., Weisberg, S.B., Wright, S., 2022. Development and application of a health-based framework for informing regulatory action in relation to exposure of microplastic particles in California drinking water. Microplast. Nanoplast. 2 (1), 12. https://doi.org/10.1186/s43591-022-00030-6.

Cornu, R., Béduneau, A., Martin, H., 2022. Ingestion of titanium dioxide nanoparticles: a definite health risk for consumers and their progeny. Arch. Toxicol. 96 (10), 2655–2686. https://doi.org/10.1007/s00204-022-03334-x.

Dhaka, V., Singh, S., Anil, A.G., Sunil Kumar Naik, T.S., Garg, S., Samuel, J., Kumar, M., Ramamurthy, P.C., Singh, J., 2022. Occurrence, toxicity and remediation of polyethylene terephthalate plastics. A review. Environ. Chem. Lett. 20 (3), 1777–1800. https://doi.org/10.1007/s10311-021-01384-8.

Dusza, H.M., van Boxel, J., van Duursen, M.B.M., Forsberg, M.M., Legler, J., Vähäkangas, K.H., 2023. Experimental human placental models for studying uptake, transport and toxicity of micro- and nanoplastics. Sci. Total Environ. 860, 160403. https://doi.org/10.1016/j.scitotenv.2022.160403.

European Commission (EC), 2022. Recommendation on the nanoparticle definition. 10-6 https://ec.europa.eu/environment/chemicals/nanotech/pdf/C_2022_3689_1_EN_ACT_part1_v6.pd.

EFSA Panel on Food Additives and Flavourings (FAF)Younes, M., Aquilina, G., Castle, L., Engel, K.H., Fowler, P., Frutos Fernandez, M.J., Fürst, P., Gundert-Remy, U., Gürtler, R., Husøy, T., Manco, M., Mennes, W., Moldeus, P., Passamonti, S., Shah, R., Waalkens-Berendsen, I., Wölfle, D., Corsini, E., Cubadda, F., De Groot, D., FitzGerald, R., Gunnare, S., Gutleb, A.C., Mast, J., Mortensen, A., Oomen, A., Piersma, A., Plichta, V., Ulbrich, B., Van Loveren, H., Benford, D., Bignami, M., Bolognesi, C., Crebelli, R., Dusinska, M., Marcon, F., Nielsen, E., Schlatter, J., Vleminckx, C., Barmaz, S., Carfí, M., Civitella, C., Giarola, A., Rincon, A.M., Serafimova, R., Smeraldi, C., Tarazona, J., Tard, A., Wright, M., 2021. Safety assessment of titanium dioxide (E171) as a food additive. EFSA J. 19 (5), e06585. https://doi.org/10.2903/j.efsa.2021.6585.

Fronza, B.M., Lewis, S., Shah, P.K., Barros, M.D., Giannini, M., Stansbury, J.W., 2019. Modification of filler surface treatment of composite resins using alternative silanes and functional nanogels. Dent. Mater. 35 (6), 928–936. https://doi.org/10.1016/j.dental.2019.03.007.

Gigault, J., El Hadri, H., Nguyen, B., Grassl, B., Rowenczyk, L., Tufenkji, N., Feng, S., Wiesner, M., 2021. Nanoplastics are neither microplastics nor engineered nanoparticles. Nat. Nanotechnol. 16 (5), 501–507. https://doi.org/10.1038/s41565-021-00886-4.

Hartmann, N.B., Hüffer, T., Thompson, R.C., Hassellöv, M., Verschoor, A., Daugaard, A.E., Rist, S., Karlsson, T., Brennholt, N., Cole, M., Herrling, M.P., Hess, M.C., Ivleva, N.P., Lusher, A.L., Wagner, M., 2019. Are we speaking the same language? Recommendations for a definition and categorization framework for plastic debris. Environ. Sci. Technol. 53 (3), 1039–1047. https://doi.org/10.1021/acs.est.8b05297.

Huang, D., Chen, H., Shen, M., Tao, J., Chen, S., Yin, L., Zhou, W., Wang, X., Xiao, R., Li, R., 2022. Recent advances on the transport of microplastics/nanoplastics in abiotic and biotic compartments. J. Hazard. Mater. 438, 129515. https://doi.org/10.1016/j.jhazmat.2022.129515.

Johnson, L.M., Mecham, J.B., Krovi, S.A., Moreno Caffaro, M.M., Aravamudhan, S., Kovach, A.L., Fennell, T.R., Mortensen, N.P., 2021. Fabrication of polyethylene terephthalate (PET) nanoparticles with fluorescent tracers for studies in mammalian cells. Nanoscale Adv. 3, 339–346. https://doi.org/10.1039/D0NA00888E.

Karakolis, E.G., Nguyen, B., You, J.B., Rochman, C.M., Sinton, D., 2019. Fluorescent dyes for visualizing microplastic particles and fibers in laboratory-based studies. Environ. Sci. Technol. Lett. 6, 334–340. https://doi.org/10.1021/acs.estlett.9b00241.

Lionetto, F., Corcione, C.E., Rizzo, A., Maffezzoli, A., 2021. Production and characterization of polyethylene terephthalate nanoparticles. Polymers (Basel) 13 (21), 3745. https://doi.org/10.3390/polym13213745.

Magrì, D., Sánchez-Moreno, P., Caputo, G., Gatto, F., Veronesi, M., Bardi, G., Catelani, T., Guarnieri, D., Athanassiou, A., Pompa, P.P., Fragouli, D., 2018. Laser ablation as a versatile tool to mimic polyethylene terephthalate nanoplastic pollutants: characterization and toxicology assessment. ACS Nano 12 (8), 7690–7700. https://doi.org/10.1021/acsnano.8b01331.

Mitrano, D.M., Beltzung, A., Frehland, S., Schmiedgruber, M., Cingolani, A., Schmidt, F., 2019. Synthesis of metal-doped nanoplastics and their utility to investigate fate and behaviour in complex environmental systems. Nat. Nanotechnol. 14 (4), 362–368. https://doi.org/10.1038/s41565-018-0360-3.

Mozetič, M., 2019. Surface modification to improve properties of materials. Materials (Basel) 12 (3), 441. https://doi.org/10.3390/ma12030441.

Nanogenotox, 2011. http://www.nanogenotox.eu/files/PDF/Deliverables/nanogenotox%20deliverable%203_wp4_%20dispersion%20protocol.pdf.

Nguyen, B., Tufenkji, N., 2022. Single-particle resolution fluorescence microscopy of nanoplastics. Environ. Sci. Technol. 56 (10), 6426–6435. https://doi.org/10.1021/acs.est.1c08480.

Paul, M.B., Stock, V., Cara-Carmona, J., Lisicki, E., Shopova, S., Fessard, V., Braeuning, A., Sieg, H., Böhmert, L., 2020. Micro- and nanoplastics -current state of knowledge with the focus on oral uptake and toxicity. Nanoscale Adv. 2 (10), 4350–4367. https://doi.org/10.1039/d0na00539h.

Pignattelli, S., Broccoli, A., Piccardo, M., Felline, S., Terlizzi, A., Renzi, M., 2021. Short-term physiological and biometrical responses of Lepidium sativum seedlings exposed to PET-made microplastics and acid rain. Ecotoxicol. Environ. Saf. 208, 111718. https://doi.org/10.1016/j.ecoenv.2020.111718.

PlasticsEurope, .. Plastics -The Facts 2021: An Analysis of European Plastics Production, Demand and Waste Data. (Accessed: on 13 September 2022); Available online https://plasticseurope.org/wp-content/uploads/2021/12/Plastics-the-Facts-2021-web-final.pdf.

Rodríguez-Hernández, A.G., Muñoz-Tabares, J.A., Aguilar-Guzmán, J.C., Vazquez-Duhalt, R., 2019. A novel and simple method for polyethylene terephthalate (PET) nanoparticle production. Environ. Sci. Nano 6 (7), 2031–2036. https://doi.org/10.1039/c9en00365g.

Roursgaard, M., Hezareh Rothmann, M., Schulte, J., Karadimou, I., Marinelli, E., Møller, P., 2022. Genotoxicity of particles from grinded plastic items in Caco-2 and HepG2 cells. Front. Public Health 10, 906430. https://doi.org/10.3389/fpubh.2022.906430.

Rubio, L., Marcos, R., Hernández, A., 2020. Potential adverse health effects of ingested micro- and nanoplastics on humans. Lessons learned from in vivo and in vitro mammalian models. J. Toxicol. Environ. Health B. Crit. Rev. 23 (2), 51–68. https://doi.org/10.1080/10937404.2019.1700598.

Rubio, L., Barguilla, I., Domenech, J., Marcos, R., Hernández, A., 2020b. Biological effects, including oxidative stress and genotoxic damage, of polystyrene nanoparticles in different human hematopoietic cell lines. J. Hazard. Mater. 398, 122900. https://doi.org/10.1016/j.jhazmat.2020.122900.

Smith, E.C., Turner, A., 2020. Mobilisation kinetics of Br, Cd, Cr, Hg, Pb, and Sb in microplastics exposed to simulated, dietary-adapted digestive conditions of seabirds. Sci. Total Environ. 733, 138802. https://doi.org/10.1016/j.scitotenv.2020.138802.

Suzuki, H., Toyooka, T., Ibuki, Y., 2007. Simple and easy method to evaluate uptake potential of nanoparticles in mammalian cells using a flow cytometric light scatter analysis. Environ. Sci. Technol. 41, 3018–3024. https://doi.org/10.1021/es0625632.

Tramis, O., Garnier, C., Yus, C., Irusta, S., Chabert, F., 2021. Enhancement of the fatigue life of recycled PP by incorporation of recycled opaque PET collected from household milk bottle wastes. Waste Manag. 125, 49–57. https://doi.org/10.1016/j.wasman.2021.02.006.

Turner, A., Filella, M., 2021. Hazardous metal additives in plastics and their environmental impacts. Environ. Int. 156, 106622. https://doi.org/10.1016/j.envint.2021.106622.

Vales, G., Rubio, L., Marcos, R., 2015. Long-term exposures to low doses of titanium dioxide nanoparticles induce cell transformation, but not genotoxic damage in BEAS-2B cells. Nanotoxicology 9 (5), 568–578. https://doi.org/10.3109/17435390.2014.957252.

Villacorta, A., Rubio, L., Alaraby, M., López-Mesas, M., Fuentes-Cebrian, V., Moriones, O.H., Marcos, R., Hernández, A., 2022. A new source of representative secondary PET nanoplastics. Obtention, characterization, and hazard evaluation. J. Hazard. Mater. 439, 129593. https://doi.org/10.1016/j.jhazmat.2022.129593.

Wu, P., Lin, S., Cao, G., Wu, J., Jin, H., Wang, C., Wong, M.H., Yang, Z., Cai, Z., 2022. Absorption, distribution, metabolism, excretion, and toxicity of microplastics in the human body and health implications. J. Hazard. Mater. 437, 129361. https://doi.org/10.1016/j.jhazmat.2022.129361.

Xu, J.L., Lin, X., Wang, J.J., Gowen, A.A., 2022. A review of potential human health impacts of micro- and nanoplastics exposure. Sci. Total Environ. 17, 158111. https://doi.org/10.1016/j.scitotenv.2022.158111.